MAGNETIC PROPERTIES OF AMORPHOUS MAGNETIC Co-BASED MICROWIRES

A. T. Savchuk[1] and S. A. Baranov[2,3]

[1]*Kazakh-British Technical University, Tolebi str. 59, Almaty, 050000 Republic of Kazakhstan*
E-mail: a.savchuk@kbtu.kz, asavchuk.kbtu@yandex.ru

[2]*Institute of Applied Physics, Academy of Sciences of Moldova, Academiei str.5, Chisinau, MD-2028 Republic of Moldova*
E-mail: baranov@phys.asm.md

[3]*Shevchenko State University, str. 25 Oktyabrya 128, Tiraspol, Republic of Moldova*

(Received May 15, 2017)

Abstract

The effect of thermal treatments on the magnetic behavior in negative (and nearly-zero) magnetostriction glass-coated amorphous microwires has been investigated. It has been shown that the magnetic properties of CoMnBSi microwires undergo significant changes during annealing both at low and high temperatures. The effect of the amorphous–nanocrystaline structure transformation has been discussed. The processes that lead to changes in the magnetic characteristics are associated with the homogenization of residual stress at a low annealing temperature and with the short-range order atomic structure relaxation at a high annealing temperature.

1. Introduction

The magnetic properties of cast glass-coated amorphous and nanocrystalline microwires (CGCANMWs) have been reviewed in [1–6]. Microwires were prepared of Co, Mn, B, and Si by the Ulitovsky–Taylor method. Magnetic microwires exhibit a large variety of magnetic behaviours; this feature is important for sensing applications. Depending on the chemical composition of the metallic core, the microwires based on Co, Fe, and Ni composites have different properties.

The geometrical characteristics (metallic core diameter and glass thickness) of the microwire depend on the physical properties of the metallic composite and the glass, the parameters of the heating inductor, and the drawing speed of the microwire. The diameter of the metallic core in these microwires can range from 0.5 to 70 μm; the glass thickness can vary from 1 to 50 μm.

$(CoMn)_{75}(BSi)_{25}$ cast amorphous glass-coated microwires are well known [1, 2]. Microwires with a wide range of anisotropy field values (H_k) of 20–1500 A/m and coercivity (H_c) of 1–20 A/m were prepared of this alloy. The magnetic characteristics of Co-based cast amorphous glass-coated microwires (with a negative magnetostriction constant) were studied. The residual stress distributions in this type of microwires determine the domain structures of cast amorphous and nanocrystalline microwires.

2. Magnetization Loops of Amorphous Microwires with Negative Magnetostriction

It is known that cast amorphous microwires with negative magnetostriction exhibit a nonrectangular hysteresis loop (see Fig. 1).

Anisotropy H_k and coercive forces H_c can be controlled by both residual and external mechanical stresses (see below).

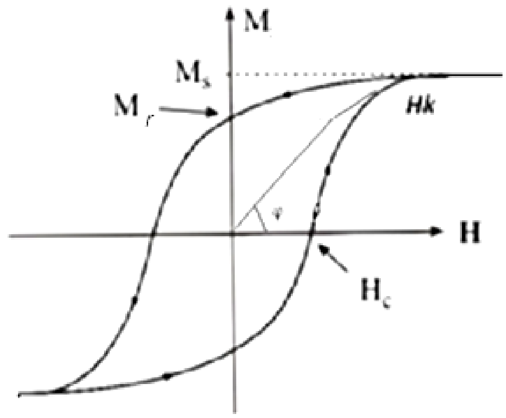

Fig. 1. Scheme of hysteresis loops of amorphous microwires with negative magnetostriction.

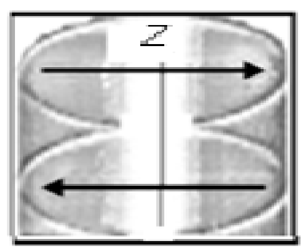

Fig. 2. Magnetic domain structure for CGCANMWs with negative magnetostriction ($\lambda_s < 0$), according to [3, 4], with the main domains oriented along the microwire radius (rouleau). There should be closure domains at the CGCANMW surface, while the walls of the main domains at the CGCANMW center are blurred and a rod is formed with longitudinal magnetization M_s and sizes $\sim A^{1/2}/M_s \sim 0.1–0.01$ μm (A is the exchange constant).

It was found that the domain structure of the Co-based cast amorphous microwire consists of orthogonal to Z domains. This result was used in [3, 4] to determine the domain structure of CGCANMWs in the case of $\lambda_s < 0$. For CGCANMWs with $\lambda_s < 0$, we obtain a result that is in contrast with the domain structure assumed, e.g., by the authors of [6] (and by some other authors), i.e., the so-called “Bamboo” magnetic domain structure. (We justify the possibility of a Bamboo-type structure, in particular, in microwires manufactured by Unitika technology in [6].) The domain structure depicted in Fig. 2 is referred to as a rouleau.

3. Experimental Setup for Measuring Magnetic Properties

A setup for measuring magnetic loops has been developed. The magnetic loops of sample (*1)* were measured by the standard induction method (Fig. 3).

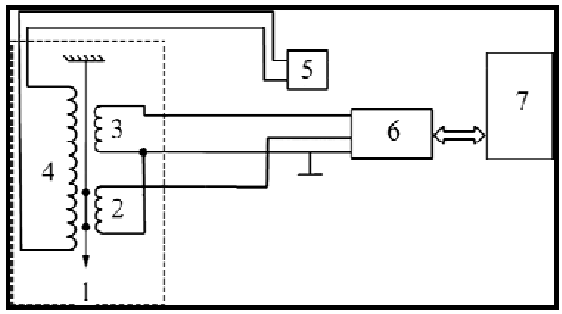

Fig. 3. Schematic circuit of a setup for hysteresis loop measurements (see text for notation).

Pickup (*2*) and compensating (*3*) coils were placed symmetrically in magnetizing coil (*4*) (connected to linear-sweep magnetic field power supply (*5*)). The analog differential signal from the pickup coil (after compensation in switching unit (*6*)) was digitized and integrated in unit (*Z*) to the shape of the integral hysteresis curve. The correctness of the integration process was verified with known reference specimens. The axial M_z–H_z hysteresis loops were measured by means of a conventional induction method at 50 Hz.

The CGCANMW with negative magnetostriction exhibits a nonrectangular hysteresis loop (see Fig. 4).

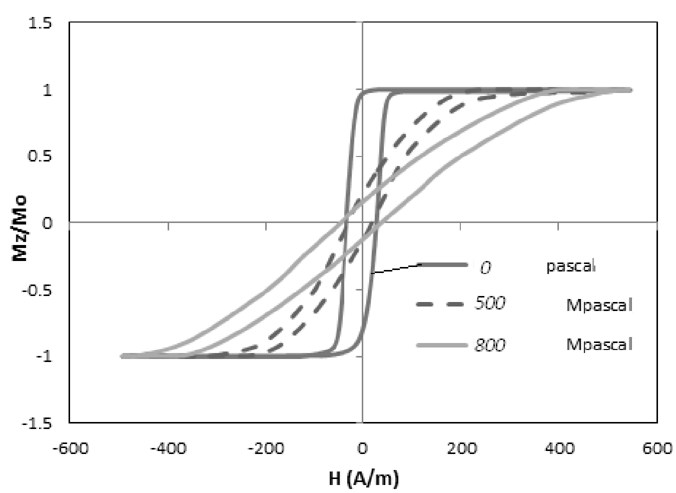

Fig. 4. Dependence of hysteresis loops of amorphous microwires with negative magnetostriction on the external mechanical stress (residual stresses are constant).

Anisotropy H_k of it can be controlled by both residual and external mechanical stresses [1–5]:

$$H_k \sim \lambda\sigma \,, \tag{1}$$

where $\sigma \sim \sigma_{ext} + \sigma_{res}$, σ_{ext} is the external mechanical stress, σ_{res} is the residual stress.

4. Residual Stresses in Microwires

In cylindrical coordinates, the residual stresses are characterized by the axial, radial, and tangential components which, to a first approximation, do not depend on radial coordinate *r* [3– 5].

(A) In the first case, where $r \sim R_m$:

$$\sigma_r = \sigma_\varphi = P = \sigma_0 \frac{k_1 x}{\left(\frac{k_1}{3}+1\right)x + \frac{4}{3}} \,, \; \sigma_z = P\frac{(k_1+1)x+2}{k_1 x+1} \,, \; x = \left(\frac{R_c}{R_m}\right)^2 - 1 \,, \tag{2}$$

where R_m is the metallic core radius of the microwire; R_c is the total radius of the microwire;

$$\sigma_0 = \varepsilon Y_m \,, \tag{3}$$

where Y_m is the Young's modulus of metal and Y_g is the Young's modulus of glass:

$$k_1 = Y_g / Y_m \,, \qquad \varepsilon = (\alpha_m - \alpha_g)(T - T^*) \,, \tag{4}$$

where α_m and α_g are the thermal expansion coefficients of the metal and glass, respectively; T^* is the effective solidification temperature of the composite microwire (when both the metallic core and the glass coating are solidified), and *T* is the experimental temperature.

A more accurate model used for residual stresses at the microwires is provided below.

The metallic strand preserves the liquid state from the strand axis up to a certain internal radius *b* (parameter *b* has a certain value depending on the defined metallic alloy composition and cooling rate), while from *b* up to R_m, where only elastic residual stresses occur, the metallic core freezes earlier.

(B) So, at $b < r < R_m$, this model gives [3, 4]:

$$\sigma_{r(1)} \approx P\left[1 - \left(\frac{b}{r}\right)^2\right], \; \sigma_{\varphi(1)} \approx P\left[1 + \left(\frac{b}{r}\right)^2\right], \; \sigma_z \approx \nu(\sigma_{r(1)} + \sigma_{\varphi(1)}) \,, \tag{5}$$

where *ν* is the Poisson's coefficient.

(C) In addition, at $r < b$, this model gives [3, 4]:

$$\sigma_{r(2)} \approx 2K_e \ln\left(\frac{r}{b}\right), \; \sigma_{\varphi(2)} \approx 2K_e\left[1 + \ln\left(\frac{r}{b}\right)\right], \; \sigma_z \approx \nu(\sigma_{r(2)} + \sigma_{\varphi(2)}) \,, \tag{6}$$

where K_e is the thermoelastic constant of metal .

Note that a rigorous solution should be obtained by lacing equations (2), (5), and (6) [3].

Formulas (2)–(6) adequately explain the experiments concerning FR and EFR [5].

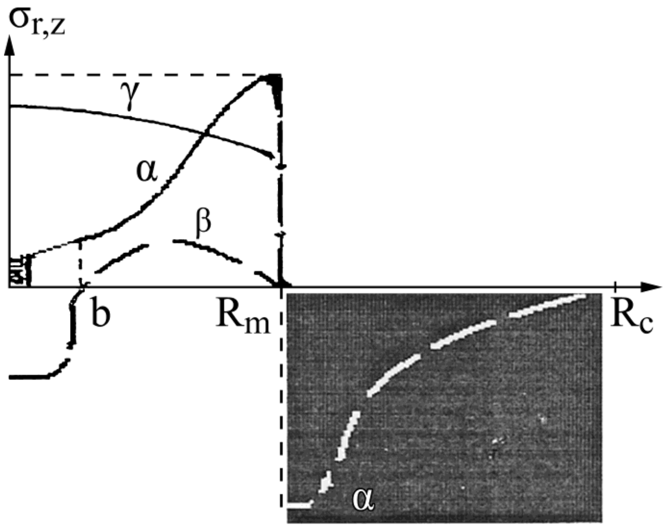

Fig. 5. Qualitative pattern of the change in residual stresses $\sigma_{r,z}$ along the microwire radius. Curve α presents the initial state of these stresses in the metal strand and in the glass (in glass it is shown by black color and a dashed line). In the metal strand, these stresses are always tensile, i.e., positive [3, 4]. The residual stresses in the silicate glass always compress the glass envelope (i.e., they are negative). Inside the plastic relaxation region, there is a section (near the strand center) where the applicability of the continuum model is violated. Curve β is a hypothetic form of residual stresses in the metal strand after removal of the glass envelope or disruption of its bond with the metal strand. For example, qualitative results of the calculation of residual stresses according to [6] (curve γ) which are different from our data are shown.

The technological parameters used for estimation in (2)–(4) are as follows:

(i) T^* is the solidification temperature of the composite in the metal/glass contact region (T^* ~ 800–1000 K), T is the room temperature; and εE_1 ~ 2 GPa is the maximum stress in the metallic core.

(ii) Technological parameter k_1 is the ratio of Young's moduli of the glass and the metal:

$$k_1 \sim 0.3\text{–}0.6.$$

(iii) Technological parameter k_1 is the ratio of Young's moduli of the glass and the metal:

$$k_1 \sim 0.3\text{–}0.6.$$

(iv) Numerical calculation indicates that, for small x values, the $\sigma_z(x)$ dependence is almost linear and exhibits saturation at $x = 10$:

$$\text{if } x < 10, \text{ then } \sigma_z \sim 2P > (\sigma_r\,,\ \sigma_\varphi \sim kx)\ ;$$

$$\text{if } x > 10, \text{ then } \sigma_z \sim 3P >> \sigma_r\,,\ \sigma_\varphi \sim P; \qquad (7)$$

$$\text{and } P \to (0.5\text{–}07)\ \sigma_0 \sim (1\text{–}2) \text{ GPa}.$$

These estimations are used for processing the results for the samples considered below.

5. Experimental Results

Figure 6 shows results of studying the dependence of anisotropy field H_k on annealing temperature.

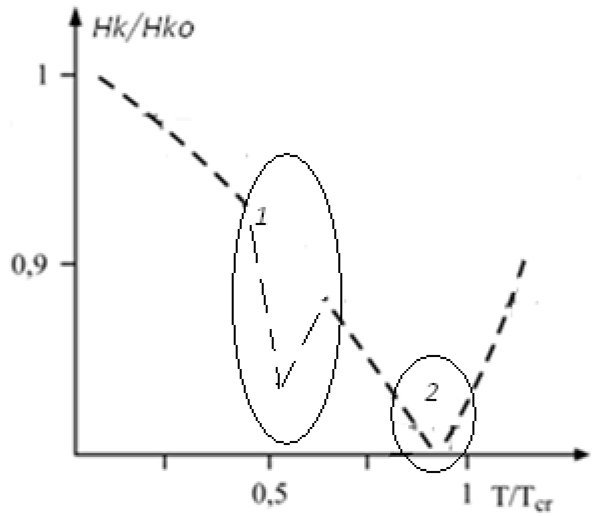

Fig. 6. Universal dependence of the relative value for anisotropy field H_k/H_{k0} (where H_{k0} is the initial anisotropy) on the heat treatment at relative temperatures T/T_{cr} (where T_{cr} is crystallization temperature of ~400°C): area *1* is the low annealing temperature region and area *2* is the high annealing temperature region.

The table shows parameters (R_m ~ 5 μm) of the studied $Co_{69}Mn_6B_{15}Si_{10}$ microwire samples.

$Co_{69}Mn_6B_{15}Si_{10}$ microwire sample parameters (R_m ~5 μm)

Samples	*X* $x = (R_g/R_m)^2 - 1.$	σ_z (MPa)	σ_φ , σ_r (MPa)
a	~1	~400	~200
b	~2	~700	~300
c	~6	~1000	~400
d	~14	~1200	~410

Figure 7 shows experimental results on the dependence of magnetic anisotropy field H_k of the studied samples on the treatment at low (area *1*) and high (area *2*) annealing temperatures *T* (°C).

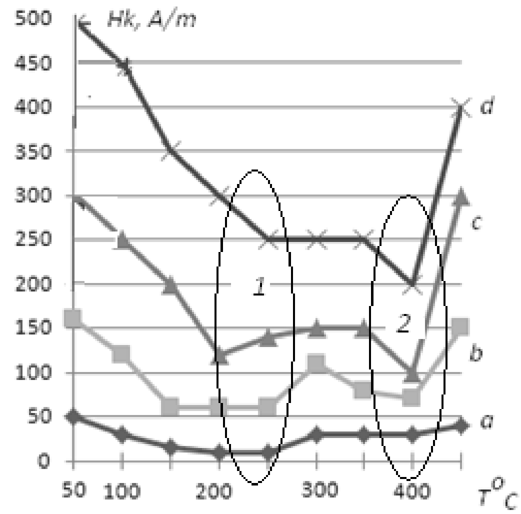

Fig. 7. Dependence of anisotropy field H_k for the $Co_{69}Mn_6B_{15}Si_{10}$ microwire samples (see table) on the treatment at low (area *1*) and high (area *2*) annealing temperatures *T* (°C). The annealing time was 30 min. Coercivity H_c of the microwire samples was ~1 A/m.

The heat treatment results are different for the two temperature regions: (*1*) at a low annealing temperature (up to 400°C) and (*2*) at an annealing temperature above 400°C.

At a low annealing temperature (up to 250°C), magnetic anisotropy H_k monotonously depends on heat treatment. A relaxation of pressure to areas A is assumed (see (2)–(4)). Permeability is determined as follows:

$$\mu_A \sim M/H_k, \quad (8)$$

where *M* is the saturation magnetisation.

An increase in the annealing temperature to 250°C leads to an increase in permeability μ_A and a decrease in magnetic anisotropy field H_k.

In an annealing temperature range of 250–400°C, the H_k values do not change (sample *d*) or slightly increase (samples *a*, *b*, and *c*). Changes in hysteresis loops (increase in the H_c values to 20 A/m) were obtained for samples *a* and *b* in this temperature region.

The electrical resistivity properties of the microwires exhibit no signs of structural transformations up to a temperature of 400°C (20 min).

After annealing at temperatures above 400°C, nonreversible changes in the structure lead to a decrease in permeability μ_A and an increase in anisotropy field H_k.

X-ray studies show that nucleation of nanocrystallites (Co_3B) begins in microwires heated around 400°C. After annealing at a temperature of 450°C, the size of effective coherent scattering regions was 5 nm. After annealing at a temperature of 500°C for 10 min, the microwire structure comprises a mixture of a saturated cobalt phase (*a* = 0.3511 nm) and a Co_3B phase. The size of effective coherent scattering regions of cubic-structure cobalt is up to 30–35 nm.

6. Conclusions

The processes that lead to a change in the magnetic anisotropy at low annealing temperatures (area *1* in Fig. 7) are associated with the homogenization of residual stress.

The processes that lead to a change in the magnetic anisotropy at high annealing temperatures are associated with a short-range order structure relaxation (in metallic core from b up to R_m).

Magnetoelastic anisotropy plays the most important role in the determination of the magnetic properties of amorphous materials (one can see it from comparison of the calculated stress values in Table 1 and initial H_k values in Fig. 7).

Satisfactory thermal processing occurs at a temperature of ~250°C.

Acknowledgments. The authors thank A.I. Dikusar for his participation in the discussion of the results.

References

[1] A. V. Torcunov, S. A. Baranov, and V. S. Larin, J. Magn. Magn. Mat. 196–197, 835, (1999).

[2] A. V. Torcunov, S. A. Baranov, V. S. Larin, and V. F. Bashev, J. Magn. Magn. Mat. 203, 231, (1999).

[3] S. A. Baranov, Surf. Eng. Appl. Electrochem. 47(4), 316, (2011).

[4] S. A. Baranov. J. Magn. Magn. Mat. 266, 278, (2003).

[5] S. A. Baranov, V. N. Berezhanskii, V. L. Kokoz, S. K. Zotov,V. S. Larin, and A.V. Torkunov, Fiz. Met. Metalloved. 67(1), 73, (1989).

[6] A. S. Antonov, V. T. Borisov, O. V. Borisov, A. F. Prokoshin, and N. A. Usov, J. Phys. D. Appl. Phys. 33, 1161, (2000).